BIOCHEMISTRY
including biophysical chemistry & molecular biology

Article

pubs.acs.org/biochemistry

Thermodynamic Analysis of the Interaction of Factor VIII with von Willebrand Factor

Jordan D. Dimitrov,*[,†,‡,§,∥] Olivier D. Christophe,[⊥] Jonghoon Kang,[#] Yohann Repessé,[†,‡,§,@] Sandrine Delignat,[†,‡,§,∥] Srinivas V. Kaveri,[†,‡,§,∥] and Sébastien Lacroix-Desmazes*[,†,‡,§,∥]

[†]Centre de Recherche des Cordeliers, Université Pierre et Marie Curie, Unité Mixte de Recherche S 872, Paris, France

[‡]Université Paris Descartes, Unité Mixte de Recherche S 872, Paris, France

[§]INSERM U872, Paris, France

[∥]Laboratoire international associé INSERM, France, and ICMR, India

[⊥]INSERM U770 and Université Paris-Sud, Le Kremlin-Bicêtre, France

[#]Department of Biology, Valdosta State University, Valdosta, Georgia 31698, United States

[@]Laboratoire d'hématologie, CHU de Caen, France

Supporting Information

ABSTRACT: Factor VIII (FVIII) is a glycoprotein that plays an important role in the intrinsic pathway of coagulation. In circulation, FVIII is protected upon binding to von Willebrand factor (VWF), a chaperone molecule that regulates its half-life, distribution, and activity. Despite the biological significance of this interaction, its molecular mechanisms are not fully characterized. We determined the equilibrium and activation thermodynamics of the interaction between FVIII and VWF. The equilibrium affinity determined by surface plasmon resonance was temperature-dependent with a value of 0.8 nM at 35 °C. The FVIII−VWF interaction was characterized by very fast association (8.56×10^6 M^{-1} s^{-1}) and fast dissociation (6.89×10^{-3} s^{-1}) rates. Both the equilibrium association and association rate constants, but not the dissociation rate constant, were dependent on temperature. Binding of FVIII to VWF was characterized by favorable changes in the equilibrium and activation entropy ($T\Delta S^\circ$ = 89.4 kJ/mol, and $-T\Delta S^\ddagger$ = −8.9 kJ/mol) and unfavorable changes in the equilibrium and activation enthalpy (ΔH° = 39.1 kJ/mol, and $\Delta H^\ddagger$ = 44.1 kJ/mol), yielding a negative change in the equilibrium Gibbs energy. Binding of FVIII to VWF in solid-phase assays demonstrated a high sensitivity to acidic pH and a sensitivity to ionic strength. Our data indicate that the interaction between FVIII and VWF is mediated mainly by electrostatic forces, and that it is not accompanied by entropic constraints, suggesting the absence of conformational adaptation but the presence of rigid "pre-optimized" binding surfaces.

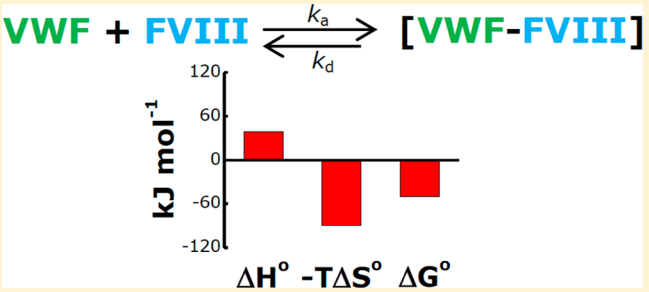

Factor VIII (FVIII) is a multidomain plasma glycoprotein and is the cofactor of activated factor IX (FIXa) in the intrinsic coagulation pathway.[1,2] Interaction of activated FVIII with FIXa at activated phospholipid surfaces expressing phosphatidylserine results in a considerable increase in the proteolytic activity of FIXa toward factor X and in the ensuing burst of thrombin generation.[3,4] The crucial role of FVIII in blood coagulation is highlighted in hemophilia A, a devastating hemorrhagic disorder that develops when the protein is lacking or is functionally impaired because of various types of abnormalities in the *F8* gene.

The full-length FVIII protein that enters the circulation consists of 2332 amino acid residues. It contains six domains (A1-A2-B-A3-C1-C2). The A domains are flanked by short polypeptide chains rich in acidic amino acid residues and designated as acidic regions a1−a3.[1,5] The mature FVIII molecule is a heterodimer of two noncovalently linked polypeptide chains: a heavy chain (A1-a1-A2-a2-B) and a light chain (a3-A3-C1-C2). The A domains of FVIII possess a β-barrel structure and are homologous in sequence and structure to each other and to the A domains of factor V and ceruloplasmin.[6−8] The C domains represent distorted β-barrels and also are homologous in sequence and structure to each other and to the C domains of factor V and proteins from the discoidin family. [7] The structures of B domain-deleted FVIII obtained by X-ray diffraction analyses revealed further details about the domain organization of FVIII.[7,8] The A domains of FVIII are closely packed and form a triangular heterotrimer with a pseudo-three-fold symmetry. The structural analyses revealed also the presence of two Cu^{2+} ions and two Ca^{2+} ions all bound to the A domains. The bound metal ions may

Received: February 19, 2012
Revised: May 6, 2012
Published: May 6, 2012

participate in the maintenance of the tertiary and quaternary structures of FVIII. The structural analyses also revealed that the C1 domain interacts tightly with the A3 domain and is thus fixed, whereas the C2 domain is loosely bound to C1 and A1 and possesses a much higher conformational flexibility.

Following its extracellular release, FVIII immediately forms a complex with von Willebrand factor (VWF).[1] This interaction plays a vital role for FVIII pro-coagulant function. VWF serves as a chaperone molecule that stabilizes FVIII and protects it from nonspecific proteolytic degradation by activated protein C and activated factor X.[1,9−12] The formation of the complex between FVIII and VWF also has a regulatory purpose as it prevents nonspecific interactions of FVIII with the phosphatidylserine-expressing membrane surfaces.[13,14] Under physiological conditions, the molar ratio of VWF to FVIII is 50:1 and the interaction is characterized by a high binding affinity at equilibrium (K_D = 0.2−0.9 nM). Hence, during its journey in blood, more than 90% of the nonactivated FVIII is in complex with VWF.[1,12] However, FVIII spontaneously dissociates from VWF after activation by proteolytic cleavage by thrombin.[15,16]

Like FVIII, VWF is a multidomain protein.[17] Its structural organization is even more sophisticated as it forms disulfide-bridged multimers that may reach a mass of 20000 kDa.[17] The significance of the interaction of VWF with FVIII is illustrated well in cases of mutations in the *vwf* gene that abrogate the interaction with FVIII, as observed in patients with type 2N von Willebrand disease.[18,19] Type 2N patients have a hemorrhagic disorder and are characterized by reduced levels of FVIII in plasma. Moreover, the exogenously administered FVIII is endowed with a considerably reduced half-life.

Despite the importance of the interaction of FVIII with VWF under physiological and pathological conditions, the molecular mechanisms that govern formation of the complex remain incompletely defined. Numerous studies have investigated the regions from FVIII and VWF involved in the binding.[20−26] The affinity and kinetics of the interaction were also investigated (reviewed in ref 12). However, the absence of structural information about the FVIII−VWF complex has precluded the understanding of the detailed topology and mechanism of the interaction. In this study, we investigated the binding of FVIII to VWF in a dynamic experimental setup. By using real-time interaction analyses, we characterized the energetic changes that occur during formation of the complex between human FVIII and human VWF. The evaluated equilibrium and activation thermodynamic changes during the binding of FVIII to VWF provide mechanistic information that may contribute to our understanding of the molecular mechanism of FVIII−VWF binding in physiology and under pathological conditions.

MATERIALS AND METHODS

Proteins. Human recombinant factor VIII Kogenate was a gift from Bayer Health Care. Human plasma-derived von Willebrand factor that was used for surface plasmon resonance was a gift from Biotest AG (Dreieich, Germany). Human plasma-derived von Willebrand factor that was used for enzyme-linked immunosorbent assay (ELISA) Wilfactin was a gift from LFB (Les Ulis, France).

Real-Time Interaction Analyses. The kinetic constants of the interactions between VWF and FVIII were determined by a surface plasmon resonance-based technique (BIAcore 2000, Biacore, GE, Uppsala, Sweden). Human plasma-derived VWF was immobilized on a C1 sensor chip using the amino coupling kit (Biacore), as described by the manufacturer. The use of dextran matrix-free C1 chips provides better stability in the presence of bivalent ions (excess Ca^{2+} ions are introduced with the FVIII preparation). The low ligand immobilization capacity of the C1 chip and the flat surface are also advantageous for studies of the interaction of high-molecular mass proteins, such as FVIII and VWF, by reducing the contribution of mass transfer and other binding artifacts. For immobilization to the sensor chip, VWF was diluted in 5 mM maleic acid (pH 3.8) to a final concentration of 100 μg/mL. Experiments were performed using HBS-P [0.01 M Hepes (pH 7.4) containing 0.15 M NaCl and 0.005% Tween 20]. Twofold dilutions of FVIII (from 10 to 0.039 nM) were injected at a rate of 10 μL/min. The association and dissociation phases were monitored for 4 min. The regeneration of the chip surface was performed by injecting a 0.5 M NaCl/0.25 M NaOH solution with a contact time no longer than 1 min. The binding to the surface of the control uncoated flow cell was subtracted from the binding to the VWF-coated flow cells.

To evaluate the effect of ionic strength on the kinetics of binding, we studied the interaction of FVIII with VWF in variants of 10 mM HEPES buffer (pH 7.2) with 0.005% Tween 20 that differ in their concentrations of NaCl (0.05, 0.1, 0.15, 0.2, 0.25, or 0.30 M). The buffers with different ionic strengths were used as running and sample dilution solutions for real-time measurements. All measurements of the ionic strength dependence of the interaction of FVIII with VWF were performed at 25 °C.

BIAevaluation version 4.1 (Biacore) was used for the estimation of the kinetic rate constants. Calculations were performed by global analysis of the experimental data using the model of Langmuir binding with a drifting baseline included in the software.

Evaluation of Binding Thermodynamics. We applied the approaches of van't Hoff and Eyring for evaluation of the equilibrium and activated complex thermodynamic parameters, respectively, of the interactions between VWF and FVIII.[27−30] All kinetic measurements were performed independently at 5, 10, 15, 20, 25, 30, and 35 °C. Equilibrium association constants obtained at different temperatures were used to build van't Hoff plots. Association and dissociation kinetic rate constants obtained at different temperatures were used to build the Arrhenius plots. The values of slopes of the plots were calculated by applying a linear regression analysis of the experimental kinetic data by using GraphPad Prism version 4 (GraphPad Inc.). Evaluation of the equilibrium thermodynamics of the interaction of FVIII with VWF was performed using the van't Hoff's equation:

$$\ln K_A = -\Delta H^\circ/RT + \Delta S^\circ/R \quad (1)$$

where R is the universal gas constant (8.3144 J mol^{-1} K^{-1}) and T is the reference temperature (298.16 K).

For the evaluation of the activation, the kinetic rate constants were used to build Arrhenius plots:

$$E_a = -\text{slope} \times R \quad (2)$$

where the slope = $\partial[\ln(k_{a/d})]/\partial(1/T)$ and E_a is the activation energy. The enthalpy, entropy, and Gibbs free energy changes characterizing the association or dissociation phases were calculated using the following equations:

$$\Delta H^{\ddagger} = E_a - RT \quad (3)$$

dx.doi.org/10.1021/bi300232d | *Biochemistry* 2012, 51, 4108−4116

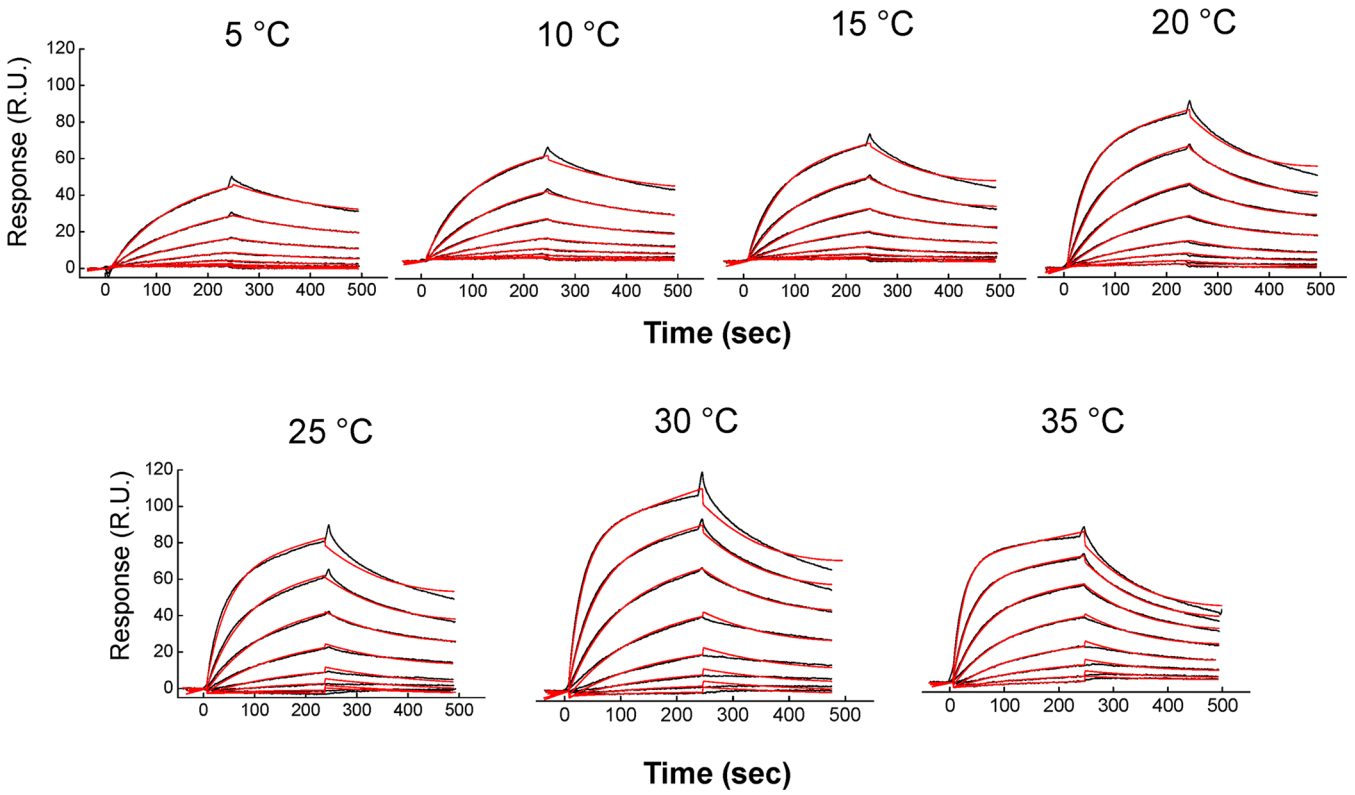

Figure 1. Effect of temperature on the binding of FVIII to VWF. Real-time interaction profiles of the binding of increasing concentrations of FVIII (0.039−5 nM) to immobilized VWF. The measurements were performed at 5, 10, 15, 20, 25, 30, and 35 °C. The experimental curves (black curves) and the curves generated by fitting data to the model of Langmuir binding with a drifting baseline by BIAevaluation (red curves) are presented. Binding intensities are expressed in resonance units (RU).

$$\ln(k_{a/d}/T) = -\Delta H^{\ddagger}/RT + \Delta S^{\ddagger}/R + \ln(k'/h) \quad (4)$$

$$\Delta G^{\ddagger} = \Delta H^{\ddagger} - T\Delta S^{\ddagger} \quad (5)$$

where T is the temperature in kelvin, k' is Boltzmann's constant, and h is Planck's constant.

The link between activation and equilibrium thermodynamics is provided with the following equations:

$$\Delta H^{\circ} = \Delta H^{\ddagger}_{\text{assoc}} - \Delta H^{\ddagger}_{\text{dissoc}}$$

$$T\Delta S^{\circ} = T\Delta S^{\ddagger}_{\text{assoc}} - T\Delta S^{\ddagger}_{\text{dissoc}}$$

$$\Delta G^{\circ} = \Delta G^{\ddagger}_{\text{assoc}} - \Delta G^{\ddagger}_{\text{dissoc}}$$

pH and Ionic Strength Dependence of the Interaction of FVIII with VWF. Ninety-six-well polystyrene plates (Nunc, Maxisorb) were coated with 5 μg/mL human VWF in PBS for 2 h at 22 °C. The plates were blocked with 1% bovine serum albumin (BSA) in PBS for 90 min at 22 °C. To study the pH dependence of the interaction between FVIII and VWF, buffers with different pH values were used. Acetate buffer (25 mM sodium acetate/acetic acid, 150 mM NaCl, and 0.05% Tween 20) was used to maintain pH values of 3.0, 3.5, 4.0, 4.5, 5.0, and 5.5. MES buffer (25 mM MES, 150 mM NaCl, and 0.05% Tween 20) was used to maintain pH values of 5.5, 6.0, and 6.5. HBS buffer (1 mM HEPES, 150 mM NaCl, and 0.05% Tween 20) was used to maintain pH values of 6.5, 7.0, 7.5, and 8.0. TBS buffer (50 mM Tris, 150 mM NaCl, and 0.05% Tween 20) was used to maintain pH values of 7.5, 8.0, 8.5, 9.0, 9.5, and 10.0. Buffers with overlapping extreme values of pH were prepared to take into account a potential effect of buffer composition on the interaction. To study of the ionic strength dependence of the binding of FVIII to VWF, 25 mM phosphate buffer (pH 7.4) and 0.05% Tween 20, containing increasing concentrations of NaCl (0, 0.0078, 0.0156, 0.0312, 0.0625, 0.125, 0.25, 0.5, and 1 M), were used. Human full-length FVIII was diluted in the different buffers to a final concentration of 2 IU/mL (approximately 0.4 μg/mL) and incubated with immobilized VWF for 1 h at 22 °C. After being extensively washed, the plates were incubated for 1 h at 22 °C with mouse monoclonal antibody 77IP52H7, specific for the A2 domain of human FVIII (a gift from LFB) diluted to 1 μg/mL in T-PBS (0.05% Tween 20). After samples had been washed, anti-mouse IgG conjugated to HRP (Southern Biotech) was added for 1 h. Immunoreactivities were revealed using the *o*-phenylenediamine substrate (Sigma-Aldrich). The absorbance at 492 nm was read after the reaction had been stopped with 2 N HCl.

RESULTS

Real-Time Interaction Analyses. We applied surface plasmon resonance to study the kinetics of the interaction of FVIII with VWF. Human plasma-derived VWF was covalently immobilized on C1 sensor chips with moderate immobilization density. The interaction of increasing concentrations (0.039−10 nM) of human recombinant FVIII was followed over time. The binding curves obtained at 25 °C indicated specific binding that approached saturation at the highest FVIII concentrations (Figure 1). The global analyses of the binding curves obtained after injection of different concentrations of FVIII allowed evaluation of the kinetic rate constants. The second-order association rate constant (k_a) obtained at 25 °C was 4.33×10^6

dx.doi.org/10.1021/bi300232d | *Biochemistry* 2012, 51, 4108−4116

M^{-1} s^{-1} (Table 1). This value implies that the formation of the complex between FVIII and VWF is a very fast process. The

Table 1. Temperature Dependence of the Kinetics of the Interaction of FVIII with VWF[a]

temp (°C)	k_a ($\times 10^6$ M^{-1} s^{-1}) (mean ± SEM)[b]	k_d ($\times 10^{-3}$ s^{-1}) (mean ± SEM)	K_A ($\times 10^8$ M^{-1})	K_D ($\times 10^{-9}$ M)
5	1.08 ± 0.01	4.41 ± 0.07	2.44	4.09
10	1.99 ± 0.02	6.74 ± 0.10	2.95	3.39
15	2.35 ± 0.01	5.91 ± 0.07	3.99	2.51
20	4.28 ± 0.03	6.87 ± 0.072	6.24	1.60
25	4.33 ± 0.04	6.58 ± 0.11	6.58	1.52
30	6.28 ± 0.05	6.7 ± 0.08	9.37	1.07
35	8.56 ± 0.05	6.89 ± 0.06	12.4	0.80

[a]Values of the kinetic rate constants (k_a and k_d) and equilibrium constants (K_A and K_D) obtained by global analyses of sensorgrams obtained after injection of FVIII (0.039−10 nM) onto the sensor chip with immobilized VWF. The binding kinetics were measured as a function of temperature. The kinetic model for Langmuir binding with a drifting baseline was used to fit the binding curves. [b]The standard error of the mean (SEM) represents the accuracy of the fit of the experimental data generated by BIAevaluation.

dissociation rate constant for the interaction (k_d) was 6.58 × 10^{-3} s^{-1}, suggesting that the interaction is characterized by a fast dissociation rate. Under our experimental conditions, the resultant equilibrium dissociation constant (K_D) was 1.52 nM.

Next, we investigated the binding of FVIII to VWF as a function of temperature. The real-time interaction profiles showed marked qualitative differences as a function of temperature (Figure 1). Thus, an increase in the temperature was associated with a gradual increase in the binding response obtained after injection of FVIII (Figure 1). Moreover, the shapes of the binding curves were affected by varying the temperature. At low temperatures, 5, 10, and 15 °C, the binding did not reach saturation, as evidenced by the linear appearance of the curve in the interaction profiles. However, at higher temperatures, the binding of FVIII approached saturation; this was the most evident at 30 and 35 °C. The qualitative differences in the binding profiles observed for the interaction of FVIII with VWF studied at different temperatures reflected quantitative differences in the binding kinetics evaluated by global analyses (Table 1). Thus, our results indicate that the association rate constant for the binding of FVIII to VWF gradually increases with an increase in temperature. The k_a value of the interaction at 5 °C was 1.08 × 10^6 M^{-1} s^{-1}, whereas at 35 °C, the estimated k_a had a value of 8.56 × 10^6 M^{-1} s^{-1}. Interestingly, the dissociation rate constant was not significantly affected over the entire temperature range except at 5 °C (Table 1). The changes in the association kinetics of binding of FVIII to VWF as a function of the temperature resulted in alterations in the binding affinity of the interaction. The plot of the equilibrium association constant versus temperature clearly shows that the increase in temperature led to a >5-fold increase in the affinity of FVIII for VWF (Figure 2A).

Analyses of Equilibrium Thermodynamics. The dependence on temperature of equilibrium affinity constants provides information about the thermodynamic changes occurring during the binding process. By using the van't Hoff approach, we evaluated the equilibrium thermodynamics of the binding of FVIII to VWF. First, the relation between the equilibrium association constant and temperature was used to

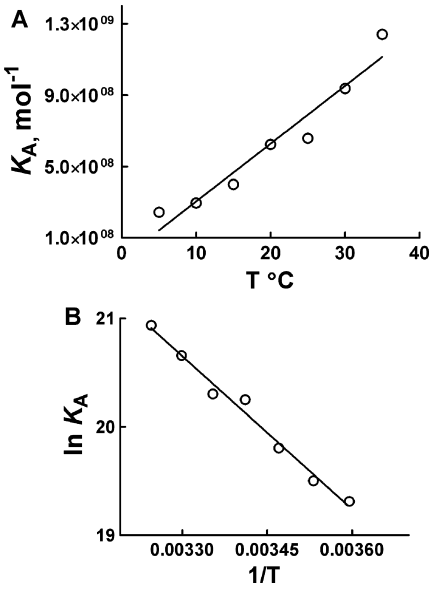

Figure 2. Temperature dependence of the equilibrium association constant of the interaction of FVIII with VWF. (A) Effect of temperature on the affinity of FVIII for VWF. The reported values of the equilibrium association constant were obtained by global analysis of the sensorgrams presented in Figure 1. The data were fit using linear regression analysis (R^2 = 0.9379). (B) van't Hoff plot of the temperature dependence of the equilibrium association constant of the interaction of FVIII with VWF. The slope of the van't Hoff plot was determined by linear regression analyses (R^2 = 0.9848).

build the van't Hoff plot [natural logarithm of the equilibrium association constant vs the reciprocal value of the temperature in kelvin (Figure 2B)]. The slope of the van't Hoff plot provides information about the changes in the equilibrium enthalpy [slope = $-\Delta H°/R$ (derived from eq 1)]. In addition, the intercept of the plot with the ordinate is linked to changes in the entropy (intercept = $\Delta S°/R$). Analysis of the van't Hoff plot for the binding of FVIII to VWF indicates that the interaction is characterized by favorable changes in the equilibrium entropy ($-\Delta S°$ = −300 ± 34 J mol^{-1}, or $-T\Delta S°$ = −89.4 kJ mol^{-1}) at the reference temperature of 298 K and unfavorable changes in the equilibrium enthalpy ($\Delta H°$ = 39.1 ± 4.5 kJ mol^{-1}). The resulting change in the equilibrium Gibbs energy was characterized by a negative sign ($\Delta G°$ = −50.3 ± 5.8 kJ mol^{-1}). When the obtained value of the free energy change was used to calculate the affinity of FVIII for VWF at 25 °C (the relation is given by the equation $\Delta G° = -RT \ln K_A$), a good agreement of the results obtained by the thermodynamic and kinetic approaches was observed ($\Delta G°$ = −50.3 kJ mol^{-1}, using a K_A of 6.58 × 10^8 M at 25 °C (Table 1)].

Analyses of Activation Thermodynamics. The relation between the temperature and kinetic rate constants allows evaluation of the activation thermodynamics of intermolecular interactions. The Arrhenius plots (Figure 3) of the binding of FVIII to VWF reveal that the association rate constant is very sensitive to changes in temperature, which is evident in the steep slope of the fitted line. The increase in the temperature correlated with an increase in the association rate (Figure 3A). In contrast, the Arrhenius plot of the dissociation rate constant revealed a much lower sensitivity to temperature (Figure 3B).

The Arrhenius plots for the rate constants of the interaction between FVIII and VWF were used to calculate the changes in the activation thermodynamic parameters (Figure 4) (derived

dx.doi.org/10.1021/bi300232d | Biochemistry 2012, 51, 4108−4116

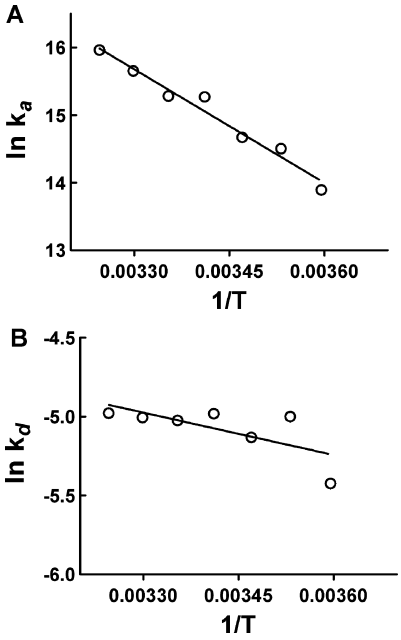

Figure 3. Temperature dependence of the kinetic rate constants of the interaction of FVIII with VWF. Arrhenius plots depicting the temperature dependency of association (A) and dissociation (B) rate constants of the binding of FVIII to VWF. The rate constants were obtained by global analyses of the sensorgrams obtained after injection of FVIII (0.039−10 nM) on immobilized VWF. The slopes of the Arrhenius plots were determined by linear regression analyses (for panel A, R^2 = 0.9701; for panel B, R^2 = 0.4882).

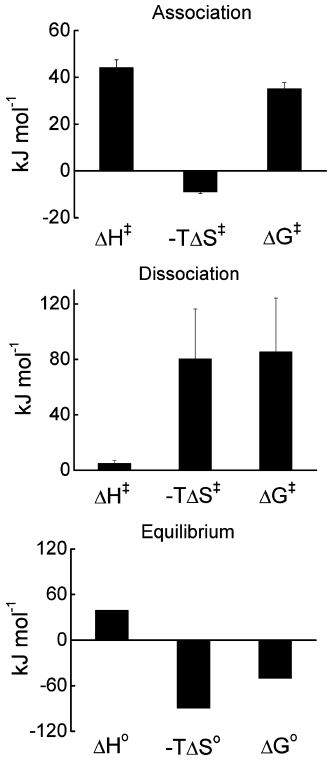

Figure 4. Activation thermodynamics of the interaction of FVIII with VWF. Changes in the activation enthalpy, entropy, and free energy during the association and dissociation phase and at equilibrium for the interaction of FVIII with VWF. Reported values were obtained by using Eyring's analyses (described in Materials and Methods) on the Arrhenius plots that are presented in Figure 3. The changes in the equilibrium thermodynamic parameters were derived from the activation thermodynamics. All thermodynamic parameters were determined using the reference temperature of 298 K. Error bars depict the standard error of the mean.

from eqs 2−5). The association phase was characterized by significant changes in enthalpy ($\Delta H^{‡}$ = 44.1 ± 3.4 kJ mol^{-1}) and much less pronounced changes in the activation entropy ($-T\Delta S^{‡}$ = −8.9 ± 0.7 kJ mol^{-1}). The resultant activation free energy change ($\Delta G^{‡}$), which represents the energetic barrier that needs to be overcome for successful association, was 35.1 ± 2.7 kJ mol^{-1}. In contrast, the dissociation phase of the interaction of FVIII with VWF was characterized by small changes in the enthalpy term ($\Delta H^{‡}$ = 4.9 ± 2.2 kJ mol^{-1}), but by considerable changes in the entropy ($-T\Delta S^{‡}$ = 80.4 ± 36 kJ mol^{-1}). The resultant value of $\Delta G^{‡}$ was equal to 85.3 ± 39 kJ mol^{-1}. Finally, we used the activation thermodynamic parameters to calculate the energetic changes for the interaction of FVIII with VWF at equilibrium (see details in Materials and Methods). The obtained values for equilibrium $\Delta H°$, $-T\Delta S°$, and $\Delta G°$ (39.2, −89.4, and −50.2 kJ mol^{-1}, respectively) were similar to the values obtained directly by van't Hoff analyses (see above), indicating good agreements of the estimation of the thermodynamics of VWF − FVIII interaction between the two approaches.

pH and Ionic Strength Dependence of the Interaction of FVIII with VWF. Changes in the thermodynamic parameters during protein−protein interactions depend on conformational changes and on noncovalent interactions between the interacting partners. To provide further understanding of the mechanism of binding of FVIII to VWF, we investigated the nature of noncovalent interactions that are responsible for the formation of a complex between VWF and FVIII. By ELISA, we first studied the binding of soluble FVIII to immobilized VWF as a function of the pH of the interaction buffer. The interaction was negligible at acidic pH values of <5 (Figure 5A). It increased rapidly above pH 5 to reach a plateau at pH 6.5, with an inflection of the pH curve occurring at pH 5.5. Interestingly, it was much less sensitive to changes in pH in the alkaline region of the titration curve, and considerable binding of FVIII to VWF was detected even at pH 10. The observed pH dependence of the interaction of FVIII with VWF may reflect the ionization behavior of different charged amino acid residues that are important for formation of the complex.

To further confirm the role of electrostatic interactions in the binding of FVIII to VWF, we performed analyses of the interaction of FVIII with VWF as a function of the ionic strength of the buffer. The binding of FVIII to VWF was sensitive to salt concentration: an increase in the ionic strength above the physiological value resulted in a concomitant decrease in the level of binding as evaluated by a solid immunosorbent assay (Figure 5B). Essentially the same ionic strength dependency of FVIII−VWF binding was observed when 25 mM phosphate buffer (pH 7.4) or 10 mM HEPES buffer (pH 7.4) and 2 mM $CaCl_2$ were used as buffering compounds (data not shown).

This result demonstrates that Ca^{2+} ions supplied with the recombinant FVIII preparation maintain the structural integrity of the molecule and no further addition of Ca^{2+} ions in the binding buffers is required.

Further, by using real-time interaction analyses and the approach described in ref 31, we studied the effect of ionic strength on the kinetics of the interaction of FVIII with VWF.

dx.doi.org/10.1021/bi300232d | *Biochemistry* 2012, 51, 4108−4116

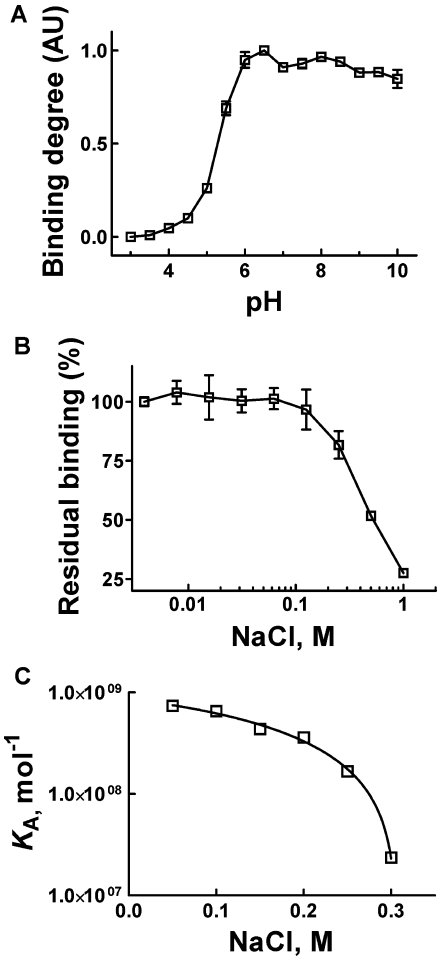

Figure 5. pH and ionic strength dependence of the interaction of FVIII with VWF. (A) The pH dependence of the binding of FVIII to VWF was studied by dilution of FVIII to 2 IU/mL in buffers at different pH values and then incubation with immobilized VWF. (B) NaCl concentration dependence of binding of FVIII to VWF. For evaluation of the ionic strength dependence of the binding of FVIII to VWF, FVIII was diluted to 2 IU/mL in 25 mM phosphate buffer (pH 7.4) that contained increasing NaCl concentrations (0.0078−1 M) and allowed to interact with immobilized VWF. In both experiments, the bound FVIII was detected by using A2-specific monoclonal antibody 77IP52H7. (C) Ionic strength dependence of the equilibrium association constant of the interaction of FVIII with VWF. The graph depicts the dependence of K_A on the concentration of NaCl in the interaction buffer. The values of K_A at different ionic strengths were obtained by global analyses of sensorgrams presented in Figure 1 of the Supporting Information.

An increase in the ionic strength resulted in a considerable decrease in the binding response as evidenced by the real-time interaction profiles (Figure 1 of the Supporting Information). Evaluation of the binding affinity revealed that an increase in the NaCl concentration of the interaction buffer from 0.05 to 0.3 M was accompanied by a 31-fold decrease in the equilibrium association constant (Figure 5C). The decrease in the affinity of FVIII for VWF as a function of ionic strength was entirely due to the decrease in the association rate constant; the dissociation rate constant of the interaction was not significantly influenced by the ionic strength (data not shown).

DISCUSSION

The functional activity of FVIII in the coagulation process depends on numerous interactions with other coagulation partners. The modular organization of the FVIII molecule mediates these different interactions. Thus, the C1 and C2 domains play a role in the binding of activated FVIII to phospholipids;[32] the A2 and A3 domains are involved in the binding to activated FIX,[7,16] and the interaction of FVIII with VWF involves the light chain and particularly the acidic a3 region and the C2 domain.[21,24,25] The binding of FVIII to VWF is critical for the normal function of FVIII.[1] The latter interaction serves a dual role: it prevents the proteolytic degradation of FVIII and inhibits the intrinsic binding promiscuity of FVIII toward other molecules, for example, phospholipids or scavenger receptors.[33−35] It can even be suggested that VWF increases the solubility of FVIII in the circulation as the latter molecule contains many hydrophobic patches[36] on its surface that can be involved in aggregation or indiscriminate interactions with other plasma molecules. Thus, the binding of FVIII to VWF has protective and regulatory functions.

The significance of this interaction for hemostasis has evoked numerous studies of the mechanism and precise topology of the binding of FVIII to VWF. The binding affinity of VWF for FVIII and the interaction kinetics have been studied using various approaches, including direct coating of VWF on plastic surfaces,[37,38] immobilization of VWF through monoclonal antibodies on beads,[39−41] analytical velocity sedimentation,[21,42] conjugation to gold nanoparticles,[39] and gel filtration.[39] Different methods provided different binding affinity values, which varied in a relatively narrow range of K_D values (from 0.2 to 0.9 nM). These studies yielded, however, more pronounced differences in the estimation of the stoichiometry of VWF−FVIII binding. The values of the kinetic rate constants of the interaction of VWF with FVIII also showed some variation in different studies. For example, by using VWF coated to Sepharose particles, Vlot and colleagues[40] estimated that FVIII binds with an association rate constant k_a of 5.9×10^6 M^{-1} s^{-1} and a dissociation rate constant k_d of 1.6×10^{-3} s^{-1}. In another study, values of k_a (6.4×10^5 M^{-1} s^{-1}) and k_d (2.3×10^{-4} s^{-1}) for binding of FVIII to covalently immobilized VWF were determined by surface plasmon resonance.[25] These discrepancies in the binding affinity and stochiometry may reflect different structural constraints introduced into the VWF molecule upon immobilization by different strategies.

The goal of this study was to provide further mechanistic information about the interaction of FVIII with VWF. We investigated the equilibrium and nonequilibrium thermodynamics of this binding as these physicochemical characteristics can provide a qualitative and quantitative description of the recognition process in terms of conformational changes, and the noncovalent forces involved in formation of the complex.[29,43−45] We studied the kinetics of binding of full-length human FVIII to covalently immobilized human VWF as a function of temperature. The results revealed that the recognition process is very sensitive to temperature. Interestingly, the variations in the interaction temperatures affected mainly the kinetics of association of FVIII with VWF, with an increase in temperature resulting in augmentation of the kinetic rate constant. It has been proposed that interactions between proteins with preoptimized binding sites generally benefit from an increase in the kinetic energy of the system (that is, an

dx.doi.org/10.1021/bi300232d | *Biochemistry* 2012, 51, 4108−4116

increase in temperature).[28,46] In contrast, the association of proteins that need conformational adaptations for formation of the complex is hampered by increases in temperature. Thus, the prominent beneficial effect of increasing temperatures on the association kinetics and the affinity of FVIII for VWF suggests that this interaction does not require significant conformational adaptation. It should also be noted that the association rate constant determined in this study, and previously measured with different assays by others, is exceptionally high for interactions between large proteins.[40,41] This fact further supports the notion that the binding of FVIII to VWF occurs via "pre-optimized" binding surfaces.

The evaluation of the equilibrium and activation thermodynamic changes that accompany the interaction of FVIII with VWF revealed the different energetic contributions to the binding process. Our data indicate that high-affinity binding of FVIII to VWF derives from favorable changes in the equilibrium entropy, as deduced by a high value of $-T\Delta S^{\circ}$ (above −89.4 kJ mol^{-1}). Changes in entropy depend on conformational and steric changes in the interacting macromolecules or in the surrounding solvent.[28,29,43,44] This contribution of entropy was partly attenuated by the unfavorable value of the equilibrium enthalpy (ΔH° = 39.1 kJ mol^{-1}) for the overall changes in affinity. Enthalpy changes depend on noncovalent interactions between binding molecules. Protein−protein interactions that are characterized by favorable changes in entropy are considered to interact with minimal conformational alterations in the polypeptide chain. It has been proposed that the driving force for formation of the intermolecular complex is mainly derived from an increase in the level of disorder, consequent to the disruption of solvatation shells on the binding surfaces.[47] When the energetic contributions for the FVIII−VWF binding process were further dissected by evaluation of the activation thermodynamic changes, we observed the absence of entropic constraints for the binding, as evidenced by the favorable changes in the association entropy ($-T\Delta S^{\ddagger}$ = −8.9 kJ mol^{-1}). Taken together, the results from equilibrium and activation changes in the entropy confirm that formation of the complex between FVIII and VWF is not accompanied by significant structural changes. The activation thermodynamics also reveal that unfavorable changes in the enthalpy of association were not attenuated by changes in enthalpy during the dissociation (as evidenced by the negligible value of dissociation $\Delta H^{\ddagger}$). This observation may be one of the explanations for the relatively low stability of the FVIII−VWF complex, which is highlighted by the fast dissociation rate constant. As enthalpy changes account for noncovalent interactions between interacting partners, these results also suggest that the energy of the noncovalent interactions responsible for maintaining the stability of the FVIII−VWF complex is relatively low. Low complex stability can be important for the regulatory function of VWF toward FVIII activity. Indeed, a high stability of the FVIII−VWF complex could hamper the dissociation of FVIII from VWF once FVIII is activated by thrombin.

The ionic strength and pH dependence analyses of the binding of FVIII to VWF reveal that the electrostatic interactions play an important role in formation of the complex. The pH dependence was characterized by a high sensitivity in the acidic region and a lack of sensitivity in the neutral and alkaline pH regions. This result indicates that ionization of charged amino acid residues plays a decisive role in the formation of the complex. The role of electrostatic interactions in the binding of FVIII to VWF was further confirmed by inhibition of the interaction at high ionic strengths. The reduction of the binding affinity observed in this study as a function of ionic strength (Figure 5C) was solely due to a decrease in the second-order association rate constant (data not shown). Together with the fact that the interaction of FVIII with VWF at physiological ionic strengths is characterized by a high association rate constant (Table 1) that exceeds 10^5 M^{-1} s^{-1} (a value suggested as a start of the diffusion-controlled regime of protein−protein associations[48]), this implies that the formation of the complex depends on long-range electrostatic steering effects.

In addition to our results, several lines of evidence suggest that electrostatic interactions may be the main driving force for formation of the FVIII−VWF complex. (1) The putative binding sites for VWF on the FVIII molecule are strongly charged; the C2 domain bears an overall positive charge, whereas the a3 domain is strongly negatively charged.[5,32] (2) Hemophilia- and von Willebrand disease-causing mutations of some charged residues in FVIII[49] or in VWF[50] have been shown to abolish binding. For example, mutation of amino acid residues D2267, D2288, R2304, R2307, and R2320 that are localized on the putative binding site for VWF on the C2 domain of FVIII was demonstrated to alter the binding of FVIII to VWF.[51−53] Moreover, mutations of these residues result in mild or severe hemophilia A.[51−53] (3) The presence of sulfated Tyr^{1680} on FVIII, which is able to establish electrostatic interactions, is indispensable for the binding of FVIII to VWF.[54] (4) Perturbation of the electrostatic properties of some charged amino acid residues on the C2 domain plays a role in the inhibition of the interaction of FVIII with VWF by some FVIII inhibitors.[49] (5) Exposure to high salt concentrations leads to dissociation of the FVIII−VWF complex.[55]

With this study, we provided information about the mechanism of the interaction of FVIII with VWF. We demonstrated that this interaction is not accompanied by entropic constraints. This could be explained by the absence of conformational adaptations during the binding process. Further studies of disease-associated mutations in the VWF−FVIII binding surfaces should provide important mechanistic information about the impact of hemophilia A- or von Willebrand disease-causing mutations on the mechanism of molecular recognition between FVIII and VWF.

■ ASSOCIATED CONTENT

Ⓢ Supporting Information

Real-time interaction profiles of the binding of FVIII to VWF as a function of ionic strength (Figure 1). This material is available free of charge via the Internet at http://pubs.acs.org.

■ AUTHOR INFORMATION

Corresponding Author

*J.D.D.: INSERM UMR 872 Equipe 16, Centre de Recherche des Cordeliers, Paris, F-75006 France; telephone, 01 44 27 82 10; fax, 01 44 27 81 94; e-mail, jordan.dimitrov@crc.jussieu.fr. S.L.-D.: INSERM UMR 872 Equipe 16, Centre de Recherche des Cordeliers, Paris, F-75006 France; telephone, 01 44 27 82 02; fax, 01 44 27 81 94; e-mail, sebastien.lacroix-desmazes@crc.jussieu.fr.

Funding

This work was supported by INSERM, CNRS, Université Pierre et Marie Curie (UPMC-Paris6), and Agence Nationale

de la Recherche (ANR-07-RIB-002-02 and ANR-07-MRAR-028-01). J.D.D. was a recipient of a fellowship from Fondation de la Recherche Médicale (Paris, France).

Notes

The authors declare no competing financial interest.

■ ACKNOWLEDGMENTS

Kogenate and Wilactin were kind gifts from Bayer (Lille, France) and LFB (Les Ulis, France), respectively.

■ REFERENCES

(1) Lenting, P. J., van Mourik, J. A., and Mertens, K. (1998) The life cycle of coagulation factor VIII in view of its structure and function. *Blood 92*, 3983−3996.

(2) Lacroix-Desmazes, S., Navarrete, A. M., Andre, S., Bayry, J., Kaveri, S. V., and Dasgupta, S. (2008) Dynamics of factor VIII interactions determine its immunologic fate in hemophilia A. *Blood 112*, 240−249.

(3) Furie, B., and Furie, B. C. (1988) The molecular basis of blood coagulation. *Cell 53*, 505−518.

(4) Mann, K. G. (1999) Biochemistry and physiology of blood coagulation. *Thromb. Haemostasis 82*, 165−174.

(5) Fay, P. J. (2006) Factor VIII structure and function. *Int. J. Hematol. 83*, 103−108.

(6) Pemberton, S., Lindley, P., Zaitsev, V., Card, G., Tuddenham, E. G., and Kemball-Cook, G. (1997) A molecular model for the triplicated A domains of human factor VIII based on the crystal structure of human ceruloplasmin. *Blood 89*, 2413−2421.

(7) Ngo, J. C., Huang, M., Roth, D. A., Furie, B. C., and Furie, B. (2008) Crystal structure of human factor VIII: Implications for the formation of the factor IXa-factor VIIIa complex. *Structure 16*, 597−606.

(8) Shen, B. W., Spiegel, P. C., Chang, C. H., Huh, J. W., Lee, J. S., Kim, J., Kim, Y. H., and Stoddard, B. L. (2008) The tertiary structure and domain organization of coagulation factor VIII. *Blood 111*, 1240−1247.

(9) Weiss, H. J., Sussman, I. I., and Hoyer, L. W. (1977) Stabilization of factor VIII in plasma by the von Willebrand factor. Studies on posttransfusion and dissociated factor VIII and in patients with von Willebrand's disease. *J. Clin. Invest. 60*, 390−404.

(10) Fay, P. J., Coumans, J. V., and Walker, F. J. (1991) von Willebrand factor mediates protection of factor VIII from activated protein C-catalyzed inactivation. *J. Biol. Chem. 266*, 2172−2177.

(11) Koppelman, S. J., van Hoeij, M., Vink, T., Lankhof, H., Schiphorst, M. E., Damas, C., Vlot, A. J., Wise, R., Bouma, B. N., and Sixma, J. J. (1996) Requirements of von Willebrand factor to protect factor VIII from inactivation by activated protein C. *Blood 87*, 2292−2300.

(12) Vlot, A. J., Koppelman, S. J., Bouma, B. N., and Sixma, J. J. (1998) Factor VIII and von Willebrand factor. *Thromb. Haemostasis 79*, 456−465.

(13) Gilbert, G. E., Drinkwater, D., Barter, S., and Clouse, S. B. (1992) Specificity of phosphatidylserine-containing membrane binding sites for factor VIII. Studies with model membranes supported by glass microspheres (lipospheres). *J. Biol. Chem. 267*, 15861−15868.

(14) Nesheim, M., Pittman, D. D., Giles, A. R., Fass, D. N., Wang, J. H., Slonosky, D., and Kaufman, R. J. (1991) The effect of plasma von Willebrand factor on the binding of human factor VIII to thrombin-activated human platelets. *J. Biol. Chem. 266*, 17815−17820.

(15) Hill-Eubanks, D. C., and Lollar, P. (1990) von Willebrand factor is a cofactor for thrombin-catalyzed cleavage of the factor VIII light chain. *J. Biol. Chem. 265*, 17854−17858.

(16) Fay, P. J. (2004) Activation of factor VIII and mechanisms of cofactor action. *Blood Rev. 18*, 1−15.

(17) Sadler, J. E. (1998) Biochemistry and genetics of von Willebrand factor. *Annu. Rev. Biochem. 67*, 395−424.

(18) Nishino, M., Girma, J. P., Rothschild, C., Fressinaud, E., and Meyer, D. (1989) New variant of von Willebrand disease with defective binding to factor VIII. *Blood 74*, 1591−1599.

(19) Mazurier, C., Dieval, J., Jorieux, S., Delobel, J., and Goudemand, M. (1990) A new von Willebrand factor (vWF) defect in a patient with factor VIII (FVIII) deficiency but with normal levels and multimeric patterns of both plasma and platelet vWF. Characterization of abnormal vWF/FVIII interaction. *Blood 75*, 20−26.

(20) Takahashi, Y., Kalafatis, M., Girma, J. P., Sewerin, K., Andersson, L. O., and Meyer, D. (1987) Localization of a factor VIII binding domain on a 34 kDa fragment of the N-terminal portion of von Willebrand factor. *Blood 70*, 1679−1682.

(21) Lollar, P., Hill-Eubanks, D. C., and Parker, C. G. (1988) Association of the factor VIII light chain with von Willebrand factor. *J. Biol. Chem. 263*, 10451−10455.

(22) Foster, P. A., Fulcher, C. A., Houghten, R. A., and Zimmerman, T. S. (1988) An immunogenic region within residues Val1670-Glu1684 of the factor VIII light chain induces antibodies which inhibit binding of factor VIII to von Willebrand factor. *J. Biol. Chem. 263*, 5230−5234.

(23) Fay, P. J., and Smudzin, T. M. (1990) Topography of the human factor VIII-von Willebrand factor complex. *J. Biol. Chem. 265*, 6197−6202.

(24) Saenko, E. L., Shima, M., Rajalakshmi, K. J., and Scandella, D. (1994) A role for the C2 domain of factor VIII in binding to von Willebrand factor. *J. Biol. Chem. 269*, 11601−11605.

(25) Saenko, E. L., and Scandella, D. (1997) The acidic region of the factor VIII light chain and the C2 domain together form the high affinity binding site for von willebrand factor. *J. Biol. Chem. 272*, 18007−18014.

(26) Spiegel, P. C., Jr., Jacquemin, M., Saint-Remy, J. M., Stoddard, B. L., and Pratt, K. P. (2001) Structure of a factor VIII C2 domain-immunoglobulin G4κ Fab complex: Identification of an inhibitory antibody epitope on the surface of factor VIII. *Blood 98*, 13−19.

(27) Myszka, D. G. (2000) Kinetic, equilibrium, and thermodynamic analysis of macromolecular interactions with BIACORE. *Methods Enzymol. 323*, 325−340.

(28) Manivel, V., Sahoo, N. C., Salunke, D. M., and Rao, K. V. (2000) Maturation of an antibody response is governed by modulations in flexibility of the antigen-combining site. *Immunity 13*, 611−620.

(29) Amzel, L. M. (2000) Calculation of entropy changes in biological processes: Folding, binding, and oligomerization. *Methods Enzymol. 323*, 167−177.

(30) Dimitrov, J. D., Lacroix-Desmazes, S., Kaveri, S. V., and Vassilev, T. L. (2007) Transition towards antigen-binding promiscuity of a monospecific antibody. *Mol. Immunol. 44*, 1854−1863.

(31) Baerga-Ortiz, A., Rezaie, A. R., and Komives, E. A. (2000) Electrostatic dependence of the thrombin-thrombomodulin interaction. *J. Mol. Biol. 296*, 651−658.

(32) Pratt, K. P., Shen, B. W., Takeshima, K., Davie, E. W., Fujikawa, K., and Stoddard, B. L. (1999) Structure of the C2 domain of human factor VIII at 1.5 Å resolution. *Nature 402*, 439−442.

(33) Lenting, P. J., Neels, J. G., van den Berg, B. M., Clijsters, P. P., Meijerman, D. W., Pannekoek, H., van Mourik, J. A., Mertens, K., and van Zonneveld, A. J. (1999) The light chain of factor VIII comprises a binding site for low density lipoprotein receptor-related protein. *J. Biol. Chem. 274*, 23734−23739.

(34) Saenko, E. L., Yakhyaev, A. V., Mikhailenko, I., Strickland, D. K., and Sarafanov, A. G. (1999) Role of the low density lipoprotein-related protein receptor in mediation of factor VIII catabolism. *J. Biol. Chem. 274*, 37685−37692.

(35) Dasgupta, S., Navarrete, A. M., Bayry, J., Delignat, S., Wootla, B., Andre, S., Christophe, O., Nascimbeni, M., Jacquemin, M., Martinez-Pomares, L., Geijtenbeek, T. B., Moris, A., Saint-Remy, J. M., Kazatchkine, M. D., Kaveri, S. V., and Lacroix-Desmazes, S. (2007) A role for exposed mannosylations in presentation of human therapeutic self-proteins to CD4+ T lymphocytes. *Proc. Natl. Acad. Sci. U.S.A. 104*, 8965−8970.

(36) Sudhakar, K., and Fay, P. J. (1996) Exposed hydrophobic sites in factor VIII and isolated subunits. *J. Biol. Chem. 271*, 23015−23021.
(37) Leyte, A., Verbeet, M. P., Brodniewicz-Proba, T., Van Mourik, J. A., and Mertens, K. (1989) The interaction between human blood-coagulation factor VIII and von Willebrand factor. Characterization of a high-affinity binding site on factor VIII. *Biochem. J. 257*, 679−683.
(38) Ganz, P. R., Atkins, J. S., Palmer, D. S., Dudani, A. K., Hashemi, S., and Luison, F. (1991) Definition of the affinity of binding between human von Willebrand factor and coagulation factor VIII. *Biochem. Biophys. Res. Commun. 180*, 231−237.
(39) Vlot, A. J., Koppelman, S. J., van den Berg, M. H., Bouma, B. N., and Sixma, J. J. (1995) The affinity and stoichiometry of binding of human factor VIII to von Willebrand factor. *Blood 85*, 3150−3157.
(40) Vlot, A. J., Koppelman, S. J., Meijers, J. C., Dama, C., van den Berg, H. M., Bouma, B. N., Sixma, J. J., and Willems, G. M. (1996) Kinetics of factor VIII-von Willebrand factor association. *Blood 87*, 1809−1816.
(41) Bendetowicz, A. V., Wise, R. J., and Gilbert, G. E. (1999) Collagen-bound von Willebrand factor has reduced affinity for factor VIII. *J. Biol. Chem. 274*, 12300−12307.
(42) Lollar, P., and Parker, C. G. (1987) Stoichiometry of the porcine factor VIII-von Willebrand factor association. *J. Biol. Chem. 262*, 17572−17576.
(43) Janin, J. (1995) Principles of protein-protein recognition from structure to thermodynamics. *Biochimie 77*, 497−505.
(44) Stites, W. E. (1997) Protein-Protein Interactions: Interface Structure, Binding Thermodynamics, and Mutational Analysis. *Chem. Rev. 97*, 1233−1250.
(45) Sundberg, E. J., and Mariuzza, R. A. (2002) Molecular recognition in antibody-antigen complexes. *Adv. Protein Chem. 61*, 119−160.
(46) Manivel, V., Bayiroglu, F., Siddiqui, Z., Salunke, D. M., and Rao, K. V. (2002) The primary antibody repertoire represents a linked network of degenerate antigen specificities. *J. Immunol. 169*, 888−897.
(47) Chothia, C., and Janin, J. (1975) Principles of protein-protein recognition. *Nature 256*, 705−708.
(48) Schreiber, G., Haran, G., and Zhou, H. X. (2009) Fundamental aspects of protein-protein association kinetics. *Chem. Rev. 109*, 839−860.
(49) Dimitrov, J. D., Roumenina, L. T., Plantier, J. L., Andre, S., Saboulard, D., Meslier, Y., Planchais, C., Jacquemin, M., Saint-Remy, J. M., Atanasov, B. P., Kaveri, S. V., and Lacroix-Desmazes, S. (2010) A human FVIII inhibitor modulates FVIII surface electrostatics at a VWF-binding site distant from its epitope. *J. Thromb. Haemostasis 8*, 1524−1531.
(50) Bowen, D. J., Standen, G. R., Mazurier, C., Gaucher, C., Cumming, A., Keeney, S., and Bidwell, J. (1998) Type 2N von Willebrand disease: Rapid genetic diagnosis of G2811A (R854Q), C2696T (R816W), T2701A (H817Q) and G2823T (C858F)—detection of a novel candidate type 2N mutation: C2810T (R854W). *Thromb. Haemostasis 80*, 32−36.
(51) Liu, M. L., Shen, B. W., Nakaya, S., Pratt, K. P., Fujikawa, K., Davie, E. W., Stoddard, B. L., and Thompson, A. R. (2000) Hemophilic factor VIII C1- and C2-domain missense mutations and their modeling to the 1.5-angstrom human C2-domain crystal structure. *Blood 96*, 979−987.
(52) Spiegel, P. C., Murphy, P., and Stoddard, B. L. (2004) Surface-exposed hemophilic mutations across the factor VIII C2 domain have variable effects on stability and binding activities. *J. Biol. Chem. 279*, 53691−53698.
(53) Vencesla, A., Corral-Rodriguez, M. A., Baena, M., Cornet, M., Domenech, M., Baiget, M., Fuentes-Prior, P., and Tizzano, E. F. (2008) Identification of 31 novel mutations in the F8 gene in Spanish hemophilia A patients: Structural analysis of 20 missense mutations suggests new intermolecular binding sites. *Blood 111*, 3468−3478.
(54) Leyte, A., van Schijndel, H. B., Niehrs, C., Huttner, W. B., Verbeet, M. P., Mertens, K., and van Mourik, J. A. (1991) Sulfation of Tyr1680 of human blood coagulation factor VIII is essential for the interaction of factor VIII with von Willebrand factor. *J. Biol. Chem. 266*, 740−746.
(55) Weiss, H. J., and Hoyer, I. W. (1973) Von Willebrand factor: Dissociation from antihemophilic factor procoagulant activity. *Science 182*, 1149−1151.